Mechanical dissipation in MoRe superconducting metal drums

Yanai, S.; Singh, V.; Yuan, M.; Gely, M. F.; Bosman, S. J.; Steele, G. A.

DOI
10.1063/1.4976831

Publication date
2017

Document Version
Final published version

Published in
Applied Physics Letters

Mechanical dissipation in MoRe superconducting metal drums

S. Yanai, V. Singh, M. Yuan, M. F. Gely, S. J. Bosman, and G. A. Steele

Citation: Appl. Phys. Lett. **110**, 083103 (2017);
View online: https://doi.org/10.1063/1.4976831
View Table of Contents: http://aip.scitation.org/toc/apl/110/8
Published by the American Institute of Physics

Mechanical dissipation in MoRe superconducting metal drums

S. Yanai, V. Singh,[a] M. Yuan, M. F. Gely, S. J. Bosman, and G. A. Steele
Department of Quantum Nanoscience, Kavli Institute of Nanoscience, Delft University of Technology, Lorentzweg 1, 2628 CJ Delft, The Netherlands

(Received 22 July 2016; accepted 6 February 2017; published online 21 February 2017)

We experimentally investigate dissipation in mechanical resonators made of a disordered superconducting thin film of a Molybdenum-Rhenium(MoRe) alloy. Electrostatically driving the drum with a resonant AC voltage, we detect its motion using a superconducting microwave cavity. From the temperature dependence of mechanical resonance frequencies and quality factors, we find evidence for non-resonant, mechanically active two-level systems (TLSs) limiting its quality factor at low temperature. In addition, we observe a strong suppression of mechanical dissipation at large mechanical driving amplitudes, suggesting an unconventional saturation of the non-resonant TLSs. These observations shed light on the mechanism of mechanical damping in superconducting drums and routes towards understanding dissipation in such devices. *Published by AIP Publishing.*
[http://dx.doi.org/10.1063/1.4976831]

Nanoelectromechanical systems have evolved into an important platform in modern information technology. They are extensively used for applications in sensing, filtering, and timing.[1] One remarkable example is cavity opto/electromechanics.[2,3] The demonstrations of the quantum ground state of mechanical resonators have opened new applications of nano-electromechanical systems (NEMS) in quantum information technology.[4,5] To this end, the approach of cavity optomechanics, which uses the interaction between light and mechanical motion, has enabled the applications of NEMS towards the near-quantum limited frequency conversion,[6,7] temporal and spectrum shaping of signals,[8] and a nearly quantum limited frequency-mixer.[9]

A common implementation of an optomechanical system is realized by coupling a superconducting drumhead resonator to a microwave cavity. For quantum-limited performance of such a coupled system, both the drumhead resonator and the superconducting cavity should have low dissipation rates. In recent years, superconducting metal drums[10] have emerged as a popular platform for microwave optomechanics. While such drums can exhibit very low dissipation, there is also a large spread in reported mechanical Q-factors[10–13] and not many reports studying the dissipation mechanisms in such devices.

Here, we explore mechanical dissipation mechanisms in such superconducting drum resonators as a function of temperature and driving amplitude. The variation in the dissipation rate and resonant frequency with temperature suggests that mechanically active two-level systems (TLSs)[14–16] play an important role, setting the dissipation in these disordered superconductors akin to acoustic studies performed earlier on superconducting glasses.[17] By varying the acoustic excitation strength, we further observe an amplitude dependent damping rate supporting the role of TLSs, similar to the observations made in superconducting microwave resonators in response to the electromagnetic field[18,19] with electrical TLSs but with an unconventional saturation of the non-resonant mechanical TLSs by the mechanical drive.

The drums studied in this letter were made using films of a superconducting alloy of Molybdenum and Rhenium (MoRe 60–40). The compatibility of MoRe with HF, oxygen plasma, and an elastic modulus of ≈1 GPa makes it an attractive candidate for making hybrid electromechanical devices.[20] The electrical properties of MoRe are well studied, establishing its disordered nature with a residual resistance ratio of approximately unity and a superconducting transition temperature of 9.2 K.[21–24] The electrical dissipation of such films in the microwave frequency domain has been characterized in earlier studies[25] and recent reports in coplanar waveguides.[26]

Fig. 1(a) shows an optical microscopy image of our complete optomechanical device. It consists of a superconducting drumhead resonator and a high-impedance microwave cavity both made of MoRe. The mechanically compliant drumhead resonator is galvanically shorted to the high-impedance microwave cavity, enabling electrostatic actuation of its motion. The microwave cavity is coupled through the drumhead to the feedline, such that its response can be accessed in a reflection measurement. Fig. 1(b) shows a scanning electron

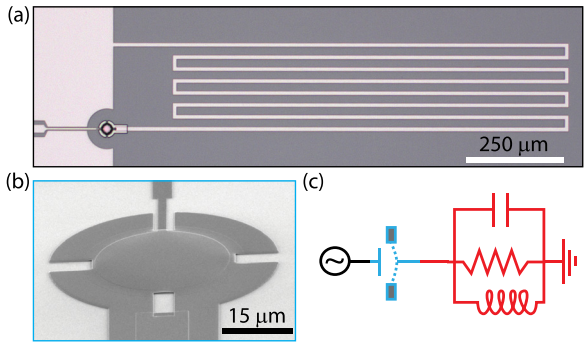

FIG. 1. Microwave cavity readout of a superconducting drum with electrostatic driving. (a) Optical microscopy image of the device. A drumhead mechanical oscillator is capacitively coupled to the microwave input port of a high impedance microwave cavity on a sapphire substrate. (b) Scanning electron microscopy image of the MoRe drumhead resonator. The drum is 30 μm in diameter and is suspended approximately 290 nm above the gate bottom electrode. (c) Device schematic diagram: the mechanical drum is capacitively coupled to the microwave input port. Motion of the drum modulates both the resonance frequency ω_c and the external coupling rate κ_e of the cavity.

[a]Present address: Department of Physics, Indian Institute of Science, Bangalore, India

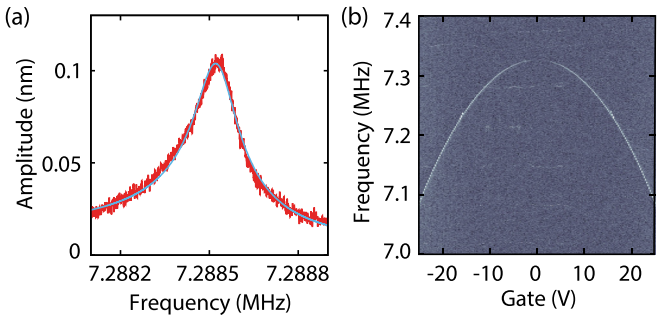

FIG. 2. Characterization of the mechanical response of the drumhead resonator. (a) Mechanical response of the MoRe drumhead resonator at 10 V of applied voltage (red curve) along with the fitted curve (light blue), yielding a quality-factor of 50 248 and a resonant frequency of 7.2885 MHz. (b) Colorscale plot of the mechanical response vs. the frequency of the RF drive signal and the DC gate voltage: the mechanical resonance frequency can be tuned over 200 kHz with ±25 V of DC gate voltage.

microscopy image of the drumhead resonator. We apply microwave signals to the cavity via a mechanically compliant capacitor. Detection of the motion of the drum occurs through its modulation of the cavity frequency, ω_c, and the external cavity decay rate, κ_e as schematically shown in Fig. 1(c).

To actuate the drumhead resonator, we apply a DC signal V_{DC} and a small RF signal V_{AC} near the mechanical resonance frequency ω_m simultaneously to the input port. Due to capacitive attraction, this signal exerts a force $C_g' V_{DC} V_{AC}$ on the drumhead resonator, where $C_g' = dC_g/dx$ is the derivative of the capacitance between the resonator and the feedline with respect to distance. In order to read out the mechanical motion, we drive the system with a microwave tone at the cavity resonance frequency ω_c. Due to electro-mechanical coupling, mechanical motion modulates the intra-cavity power, creating sideband signals in the reflected signal. The sideband signals are amplified and then mixed down with a local oscillator tone at the cavity resonance frequency. The signal is further amplified and sent to a spectrum analyzer. Using the mechanical resonator as the coupling capacitor to the cavity enables both the direct electrostatic actuation of the motion and tuning of the mechanical resonance frequency using voltages applied to the feedline.

The fabricated samples are placed in a radiation-tight box and cooled down to 20 mK in a dilution refrigerator with sufficient attenuation at each temperature stage to thermalize the microwave signals (see supplementary material (SM) for measurement chain schematic). We first begin by characterizing the microwave cavity. The microwave cavity has a resonance frequency of $\omega_c/2\pi = 6.30 \times 10^9\,\mathrm{s}^{-1}$, an external coupling rate of $\kappa_e/2\pi = 31.0 \times 10^6\,\mathrm{s}^{-1}$, and an internal dissipation rate of $\kappa_i/2\pi = 25.8 \times 10^6\,\mathrm{s}^{-1}$ (see supplementary material for detailed measurements). The red curve in Fig. 2(a) shows the measured mechanical response of the resonator along with a skewed-Lorentzian fit (light-blue line). The slight asymmetry in the measured homodyne signal arises from the finite electrical isolation and is discussed in the supplementary material. From the fit, we find a mechanical resonance frequency of $\omega_m/2\pi = 7.2885 \times 10^6\,\mathrm{s}^{-1}$ with a quality-factor Q_m of 50×10^3 at $V_{DC} = 10$ V. Fig. 2(b) shows a colorscale plot of the measured homodyne signal as a function of frequency of the RF signal used for mechanical driving and DC gate voltage applied to the feedline using a bias tee. The sharp

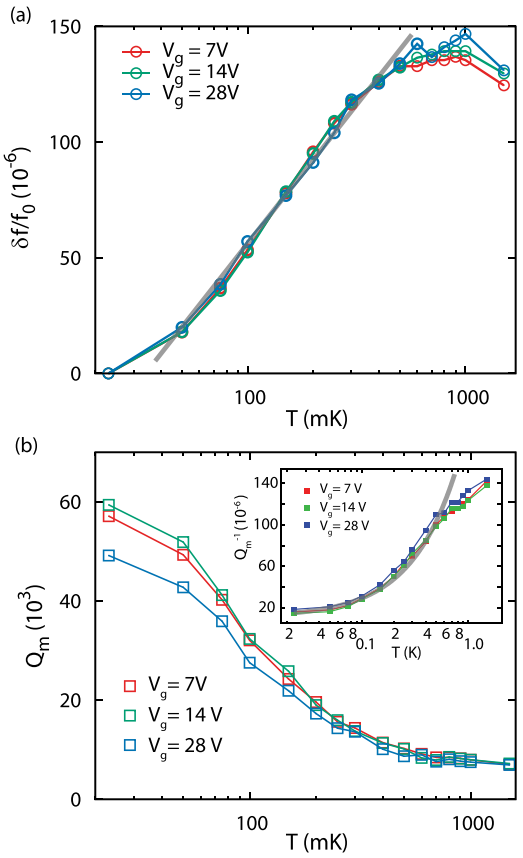

FIG. 3. Temperature dependence of (a) normalized relative frequency shift $\delta f = (f_0(T) - f_0(23\,\mathrm{mK}))/f_0(23\,\mathrm{mK})$ and (b) the mechanical quality factor. The mechanical quality-factor is determined from fitting to a Lorentzian function. Measurements are taken at three different voltages 7, 14, and 28 V. The inset shows the plot of inverse quality-factor Q_m^{-1}. The gray lines are the numerical fits to the data.

change in color reflects the mechanical resonance frequency. As the DC voltage is tuned away from zero, the mechanical resonance frequency decreases approximately quadratically, showing the well-studied capacitive softening effect.[27] The mechanical frequency is pulled by 200 kHz for gate voltages of 20 V. The mechanical signal is no longer visible around zero gate voltage due to the vanishing electrostatic force.

In Fig. 3, we investigate the temperature dependence of the mechanical response from 23 mK to 1.5 K. We measured the mechanical resonance frequencies and the quality-factors at different temperatures and at different applied DC voltages, $V_g = 7$, 14, and 28 V. Fig. 3(a) shows the normalized shift in the resonance frequency for various temperature points. As the temperature is increased, the resonance frequency increases logarithmically up to a cross-over temperature of ≈900 mK. At higher temperatures, we see a slight drop in the resonance frequency. Fig. 3(b) shows the quality-factor Q_m change as a function of temperature. As the temperature is increased from 23 mK, Q_m shows a sharp decrease for all gate voltages. Above the approximate cross-over temperature observed in the mechanical frequency, Q_m stops decreasing and saturates at a value around 10 000.

The logarithmic increase in the frequency shift suggests the presence of two-level systems.[16,17,28–30] TLSs can have a very broad spectral distribution.[31] At temperatures $k_B T \gg \hbar\omega_m$, the resonant TLSs are expected to be saturated

and not able to contribute to mechanical dissipation. However, coupling of the mechanical motion to higher energy, off-resonant TLSs can still have a significant contribution to the frequency shift. Comparing results at three different voltages, the normalized shifts are independent of mechanical resonant frequency below the cross over temperature. Such a temperature dependence can also be interpreted in the context of a TLS model: at high temperatures, part of the mechanical restoring force arises from the dispersive shift of the thermal population of the high frequency TLSs. Beyond the cross-over temperature, these TLSs decouple from the mechanics due to either the changes of their thermal populations or the relaxation rate. As the TLSs are decoupled, the mechanical spring constant reduces, giving a lower mechanical frequency. For an off-resonant dispersive interaction, the normalized frequency shift is expected to scale as $\delta f/f_0 = C_s \log(T/T_0)$, where C_s is a constant proportional to the filling factor and TLS loss tangent.[31] For the fit shown in Fig. 3(a), we find $C_s \approx 5.3 \times 10^{-5}$, similar to previously reported values for mechanical TLSs in disordered superconducting films.[17,32]

To compare the behavior of dissipation with the frequency shift, we plot Q_m^{-1} in the subpanel of Fig. 3(b). In lower temperature ranges, we observe an increase in the mechanical dissipation rate with temperature, which slows down as the temperature approaches ≈700 mK. As discussed above, the interaction with resonant TLSs can be neglected due the low frequency of the drum ($k_B T \gg \hbar\omega_m$). Non-resonant TLSs, however, can also result in dissipation due to the lag between the dispersive shift of their energies due to the mechanical coupling and their equilibration time with the bath. The contribution of the off-resonant interaction to the damping scales as $Q_m^{-1} = C_s \frac{\Gamma(T)}{\omega_m}$ for $\omega_m > \Gamma(T)$, where Γ is the TLS relaxation rate.[31] As shown in Fig. 3(b), the numerical fits to the mechanical dissipation rate suggest that the TLS relaxation rate increases linearly with the temperature.

In Fig. 4, we explore the saturation effects of the TLSs in these drums by applying a large mechanical driving force. To increase the acoustic excitation strength, we varied the *AC* driving voltage for mechanical actuation. Fig. 4(a) shows mechanical responsivity (also known as mechanical susceptibility and referred to as normalized response) at different driving voltages in the limits of linear restoring force (Lorentzian mechanical response) and non-linear restoring forces (Duffing response from non-linear spring effects). At higher amplitude drive forces, the responsivity increases, indicating the presence of a nonlinear damping term,[16] but with a negative coefficient, similar to recent reports with multilayer graphene resonators.[33] Note also, however, that the net damping, including both linear and nonlinear terms, is still positive. We also note that the response observed here has the opposite sign to the nonlinear damping terms to the commonly observed in NEMS devices.[16] In the regime of linear restoring forces, we can quantify the decrease in the damping with driving force by fitting the mechanical response to extract an effective power-dependent quality factor, Fig. 4(b). Similar negative nonlinear damping characteristics were also observed in a similar second device (data included in the supplementary materials). Although a qualitatively similar increase in responsivity could also arise from

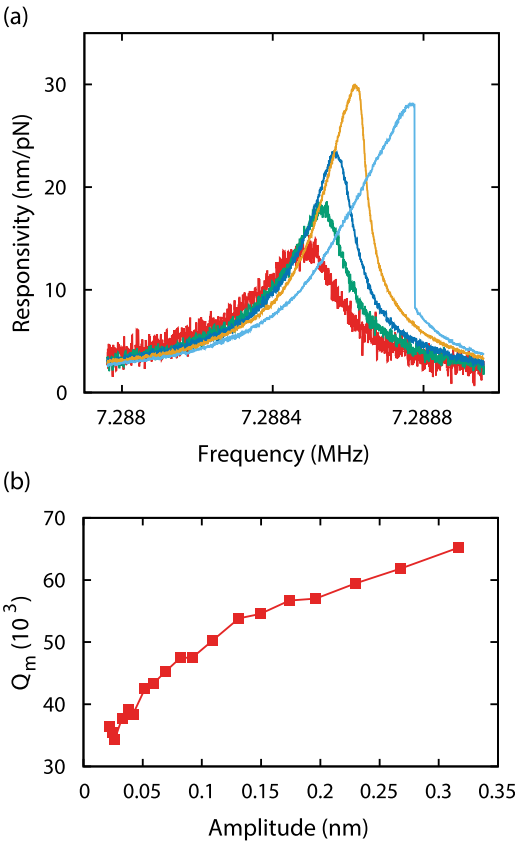

FIG. 4. Negative nonlinear damping of a superconducting metal drum. (a) Mechanical responsivity (x_0/F_0) (normalized amplitude) of the drum for different driving forces (Red-light blue: 2.9, 5.8, 11.2, 29.3, and 82.8 pN). As the driving force is increased (red-dark blue), the responsivity of the drum on resonance increases, indicating an increase in the mechanical quality-factor. As the drum is driven into the regime of nonlinear restoring forces (yellow), the Q_m continues to increase, and at higher powers, the Q_m in the nonlinear regime begins to drop, as can be seen by the decreased responsivity of the light blue curve. (b) Mechanical quality-factor as a function of mechanical amplitudes. In the regime of linear restoring forces (before the onset of a Duffing response), Q_m is extracted by fitting the curves with a Lorentzian curve with a Fano correction. A 3 dB uncertainty in power reaching at the sample results in 25% uncertainty in the estimation of mechanical amplitude.

electrostatic parametric gain, we find that the power of the AC drive voltage is at least three orders of magnitude to small to explain our observations by parametric effects.

While a decrease in the mechanical damping shown in Figure 4 appears similar to the case of the saturation of resonant TLSs in superconducting microwave cavities, such saturation effects are not typically observed when the interaction with the TLSs is non-resonant as the non-resonant drive is not able to excite the TLSs directly. The observation presented here of decreased damping at large mechanical excitation, also recently reported for the case of graphene resonators, suggests that a strongly non-equilibrium population of high frequency TLSs is induced by the low frequency driving forces, for example, by either strong higher-order excitation processes or a decoupling of the non-resonant TLSs from their bath.

In conclusion, we have studied dissipation in mechanical drumhead resonators made of a superconducting alloy of MoRe. The temperature dependence of the dissipation and resonant frequency strongly suggests the presence of

mechanically active TLSs in these disordered superconducting thin film mechanical resonators. At low temperatures, the main contribution to dissipation and frequency shift stems from the dispersive interaction with TLSs, with slow relaxation rates <7 MHz. We further explored the mechanical dissipation while varying the strength of the acoustic field and observed an amplitude dependent damping, suggesting a non-equilibrium population of non-resonant TLSs induced by the mechanical drive.

See supplementary material for device fabrication steps, cavity characterization, measurement setup, and estimation of the mechanical amplitude.

The work was supported by the Dutch Science Foundation (NWO/FOM).

[1]K. L. Ekinci and M. L. Roukes, Rev. Sci. Instrum. **76**(6), 061101 (2005).
[2]M. Aspelmeyer, T. J. Kippenberg, and F. Marquardt, Rev. Mod. Phys. **86**(4), 1391–1452 (2014).
[3]M. Metcalfe, Appl. Phys. Rev. **1**(3), 031105 (2014).
[4]J. D. Teufel, T. Donner, D. Li, J. W. Harlow, M. S. Allman, K. Cicak, A. J. Sirois, J. D. Whittaker, K. W. Lehnert, and R. W. Simmonds, Nature **475**(7356), 359–363 (2011).
[5]J. Chan, T. P. M. Alegre, A. H. Safavi-Naeini, J. T. Hill, A. Krause, S. Groeblacher, M. Aspelmeyer, and O. Painter, Nature **478**(7367), 89–92 (2011).
[6]R. W. Andrews, R. W. Peterson, T. P. Purdy, K. Cicak, R. W. Simmonds, C. A. Regal, and K. W. Lehnert, Nat. Phys. **10**(4), 321–326 (2014).
[7]J. Bochmann, A. Vainsencher, D. D. Awschalom, and A. N. Cleland, Nat. Phys. **9**(11), 712–716 (2013).
[8]R. W. Andrews, A. P. Reed, K. Cicak, J. D. Teufel, and K. W. Lehnert, Nat. Commun. **6**, 10021 (2015).
[9]F. Lecocq, J. B. Clark, R. W. Simmonds, J. Aumentado, and J. D. Teufel, Phys. Rev. Lett. **106**, 043601 (2016).
[10]J. D. Teufel, D. Li, M. S. Allman, K. Cicak, A. J. Sirois, J. D. Whittaker, and R. W. Simmonds, Nature **471**(7337), 204–208 (2011).
[11]J. Suh, M. D. Shaw, H. G. LeDuc, A. J. Weinstein, and K. C. Schwab, Nano Lett. **12**(12), 6260–6265 (2012).
[12]E. E. Wollman, C. U. Lei, A. J. Weinstein, J. Suh, A. Kronwald, F. Marquardt, A. A. Clerk, and K. C. Schwab, Science **349**(6251), 952–955 (2015).
[13]J.-M. Pirkkalainen, E. Damskägg, M. Brandt, F. Massel, and M. Sillanpää, Phys. Rev. Lett. **115**(24) 243601 (2015).
[14]P. W. Anderson, B. I. Halperin, and C. M. Varma, Philos. Mag. **25**(1), 1–9 (1972).
[15]W. A. Phillips, Rep. Prog. Phys. **50**(12), 1657 (1987).
[16]M. Imboden and P. Mohanty, Phys. Rep. **534**(3), 89–146 January (2014).
[17]A. K. Raychaudhuri and S. Hunklinger, Z. Phys. B: Condens. Matter **57**(2), 113–125 (1984).
[18]J. Gao, M. Daal, A. Vayonakis, S. Kumar, J. Zmuidzinas, B. Sadoulet, B. A. Mazin, P. K. Day, and H. G. Leduc, Appl. Phys. Lett. **92**(15), 152505 (2008).
[19]D. P. Pappas, M. R. Vissers, D. S. Wisbey, J. S. Kline, and J. Gao, IEEE Trans. Appl. Supercond. **21**(3), 871–874 (2011).
[20]T. Leonhardt, Carlén, J.-C., M. Buck, C. R. Brinkman, W. Ren, and C. O. Stevens, AIP Conf. Proc. **458**, 685–690 (2016).
[21]E. Lerner, J. G. Daunt, and E. Maxwell, Phys. Rev. **153**(2), 487–492 (1967).
[22]V. A. Seleznev, M. A. Tarkhov, B. M. Voronov, I. I. Milostnaya, V. Y. Lyakhno, A. S. Garbuz, M. Y. Mikhailov, O. M. Zhigalina, and G. N. Gol'tsman, Supercond. Sci. Technol. **21**(11), 115006 (2008).
[23]S. Sundar, L. S. Sharath Chandra, V. K. Sharma, M. K. Chattopadhyay, and S. B. Roy, AIP Conf. Proc. **1512**(1), 1092–1093 (2016).
[24]M. Aziz, D. C. Hudson, and S. Russo, Appl. Phys. Lett. **104**(23), 233102 (2014).
[25]J. Yasaitis and R. Rose, IEEE Trans. Magn. **11**(2), 434–436 (1975).
[26]V. Singh, B. H. Schneider, S. J. Bosman, E. P. J. Merkx, and G. A. Steele, Appl. Phys. Lett. **105**(22), 222601 (2014).
[27]I. Kozinsky, H. W. C. Postma, I. Bargatin, and M. L. Roukes, Appl. Phys. Lett. **88**(25), 253101 (2006).
[28]M. Imboden and P. Mohanty, Phys. Rev. B **79**(12), 125424 (2009).
[29]F. Hoehne, Y. A. Pashkin, O. Astafiev, L. Faoro, L. B. Ioffe, Y. Nakamura, and J. S. Tsai, Phys. Rev. B **81**(18), 184112 (2010).
[30]A. Venkatesan, K. J. Lulla, M. J. Patton, A. D. Armour, C. J. Mellor, and J. R. Owers-Bradley, Phys. Rev. B **81**(7), 073410 (2010).
[31]*Tunneling Systems in Amorphous and Crystalline Solids*, edited by P. Esquinazi (Springer, Berlin Heidelberg, 1998).
[32]P. Esquinazi, H. M. Ritter, H. Neckel, G. Weiss, and S. Hunklinger, Z. Phys. B: Condens. Matter **64**(1), 81–93 (1986).
[33]V. Singh, O. Shevchuk, Y. M. Blanter, and G. A. Steele, Phys. Rev. B **93**, 245407 (2016).